Neuron 52, 159–168, November 9, 2006 ©2006 Elsevier Inc. DOI 10.1016/j.neuron.2006.06.036

The TRPM7 Ion Channel Functions in Cholinergic Synaptic Vesicles and Affects Transmitter Release

Grigory Krapivinsky,[1] Sumiko Mochida,[3] Luba Krapivinsky,[1] Susan M. Cibulsky,[1] and David E. Clapham[1,2,*]
[1] Howard Hughes Medical Institute
Cardiology
Children's Hospital Boston
1309 Enders Building
320 Longwood Avenue
[2] Department of Neurobiology
Harvard Medical School
Boston, Massachusetts 02115
[3] Department of Physiology
Tokyo Medical University
Tokyo 160-8402
Japan

Summary

A longstanding hypothesis is that ion channels are present in the membranes of synaptic vesicles and might affect neurotransmitter release. Here we demonstrate that TRPM7, a member of the transient receptor potential (TRP) ion channel family, resides in the membrane of synaptic vesicles of sympathetic neurons, forms molecular complexes with the synaptic vesicle proteins synapsin I and synaptotagmin I, and directly interacts with synaptic vesicular snapin. In sympathetic neurons, changes in TRPM7 levels and channel activity alter acetylcholine release, as measured by EPSP amplitudes and decay times in postsynaptic neurons. TRPM7 affects EPSP quantal size, an intrinsic property of synaptic vesicle release. Targeted peptide interference of TRPM7's interaction with snapin affects the amplitudes and kinetics of postsynaptic EPSPs. Thus, vesicular TRPM7 channel activity is critical to neurotransmitter release in sympathetic neurons.

Introduction

Nonselective cationic channels of the TRP ion channel family participate in the sensation of pain, heat, and taste, and in neuronal plasticity (Clapham, 2003; Ramsey et al., 2006). Although the function of many TRP channels is still elusive, it is assumed that their main role is acting as divalent ion conductors through the plasma membrane. Ion channel proteins are commonly observed in both the plasma membrane and on intracellular organelles, but justifiably their localization on internal membranes is usually assumed to be as cargo in transit to the plasma membrane. Notable exceptions are the well-established endoplasmic reticular Ca^{2+}-release channels (IP_3 and ryanodine receptors), several ClC chloride channels required for acidification of synaptic vesicles (Jentsch et al., 2005), and the only known yeast TRP channel (Palmer et al., 2001). Mucolipins (TRPML channels) are presumed intracellular vesicular channels (Di Palma et al., 2002; LaPlante et al., 2002), but their function in vesicles is not well understood.

Neurotransmitter vesicles release their cargoes by fusion with the plasma membrane followed by diffusion of their contents into the intercellular space. The fusion process itself is not completely understood, but involves a complex of proteins with specialized functions that allow them to achieve close approximation of the vesicle to the plasma membrane and sense changes in [Ca^{2+}] that trigger rapid fusion (Sudhof, 2004). Although neurotransmitter release requires ion channels, ion channels are best known for their function as the plasma membrane mediators of the timing and entry of Ca^{2+} into the cell, which in turn triggers vesicle fusion. Functional ion channels have been recorded in preparations of synaptic vesicles (Yakir and Rahamimoff, 1995; Kelly and Woodbury, 1996), and a few well-established plasma membrane channels have been proposed to localize to vesicles and regulate their ionic equilibrium (Ehrenstein et al., 1991; Grahammer et al., 2001), but their molecular identities and role in neurotransmitter release has not yet been established. The ClC-3 chloride channel is present in synaptic vesicles, but mice in which this gene had been deleted did not exhibit abnormalities in synaptic transmission in hippocampal slices (Stobrawa et al., 2001).

In summary, there are unsolved major questions about the presence and function of ion channels in vesicles. What is the complement of ion channels in the neurotransmitter vesicle, and are these channels important for neurotransmitter release? During studies of the TRPM7 protein, we noticed that it was present in synaptic vesicles and bound to several proteins of the synaptic vesicle fusion apparatus. TRPM7 is an ion channel that is permeant to monovalent cations, Ca^{2+}, and Mg^{2+}, and it is required for cell viability, but little is known about its biological function (Clapham, 2003; Ramsey et al., 2006). Here we demonstrate TRPM7's localization to synaptic vesicles of sympathetic neurons and explore its role in synaptic transmission.

Results

TRPM7 Is Localized to Synaptic Vesicle Membranes in Sympathetic Neurons

In an attempt to understand the function of TRPM7, we set out to identify proteins that interact with TRPM7 using yeast two-hybrid screening. Evolutionarily conserved protein fragments of the human TRPM7 N- and C-terminal cytoplasmic domains were chosen as baits. Screening of a human brain library with bait containing a portion of the TRPM7 N terminus (amino acids 87–326 of Q96QT4) bound full-length snapin protein (O95295) as a potential TRPM7 interactor. Snapin is a ubiquitously expressed, 15 kDa protein implicated in vesicle fusion (Buxton et al., 2003). The protein is reportedly highly enriched in purified synaptic vesicles (Ilardi et al., 1999) and affects the binding of synaptotagmin to SNAREs, and when phosphorylated by protein kinase A, it

*Correspondence: dclapham@enders.tch.harvard.edu

enhances the efficacy of synaptic transmission (Chheda et al., 2001; Thakur et al., 2004).

Our finding of the interaction of snapin with TRPM7, and snapin's putative role in neurotransmitter release, motivated us to test whether TRPM7 functions in synaptic transmission. To determine whether TRPM7 was expressed in a synaptic compartment, we measured TRPM7 content in purified rat brain synaptosomes and synaptic vesicles by western blotting. Figure 1A shows that TRPM7 is enriched in a synaptic vesicle preparation compared with crude brain microsomes and purified synaptosomes, and is absent in postsynaptic densities. This finding suggests that TRPM7 is situated in the membrane of synaptic vesicles. To confirm that TRPM7 resides in synaptic vesicles, we immunoprecipitated TRPM7 from a purified synaptic vesicle preparation and probed these precipitates for synaptic vesicle-specific proteins. The synaptic vesicle preparation was essentially free of plasma membrane and nonvesicular components of SNARE as demonstrated by the absence of Na, K-ATPase, a plasma membrane marker (Figure 1A), and SNAP25 and syntaxin (see Figure S1 in the Supplemental Data). Both synaptotagmin I and synapsin I are primarily localized in neuronal synaptic vesicles (Sudhof, 2002; Greengard et al., 1994). Figure 1B shows that TRPM7 coimmunoprecipitated the synaptic vesicle proteins synaptotagmin I and synapsin I. Reverse immunoprecipitation with synaptotagmin I and synapsin I antibodies also showed specific coimmunoprecipitation of TRPM7 with these proteins (Figure 1B). VAMP2, another synaptic vesicle-specific protein, was not bound to TRPM7 immunoprecipitated from brain (Figure 1B), and this protein served as an additional negative control for the specificity of TRPM7's interaction with synaptotagmin I and synapsin I.

The experiments so far supported TRPM7's localization to synaptic vesicles, but did not address the type of neuron expressing TRPM7 in their synaptic vesicles. Confocal immunofluorescence techniques were used to examine the distribution of TRPM7 in neurons. TRPM7 was not observed in synapses of mature hippocampal neurons (2 to 3 weeks in vitro; data not shown). However, TRPM7 was highly expressed and colocalized with the presynaptic marker synaptophysin in the neuromuscular junction (Figure 1C), suggesting that TRPM7 is present in the terminals of motor neurons. We reasoned that TRPM7 might be confined to synapses of neurons secreting positively charged neurotransmitters, such as acetylcholine, rather than synapses of neurons secreting the negatively charged glutamate and GABA neurotransmitters. Indeed, we found TRPM7 labeling (by two distinct antibodies) in varicosities of the processes of superior cervical ganglion (SCG) sympathetic neurons (Figure 1D), onion-shaped structures that are packed with synaptic vesicles (Bennett, 1972; Buckley and Landis, 1983; Jackson and Cunnane, 2001). TRPM7-expressing, cultured SCG neurons were immunogold-labeled with TRPM7 antibody, and clearly show TRPM7 inside the onion-shaped varicosity (Figure 2A). A magnified view suggests that TRPM7 is restricted to the membrane of the synaptic vesicles in these varicosities (Figure 2B). This labeling was specific since antibody preabsorption with antigen blocked vesicular labeling, and mitochondria adjacent to these synaptic vesicles were not labeled (Figures 2B and 2C). Most significantly, TRPM7 was not detected in the plasma membrane of the varicosities.

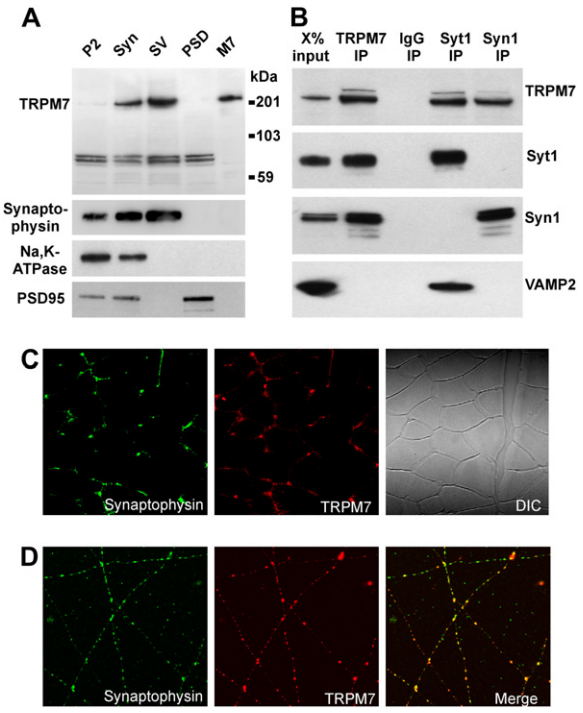

Figure 1. TRPM7 Is a Synaptic Vesicle Protein Localized in the Neuromuscular Junction and Presynapses of Sympathetic Neurons

(A) TRPM7 is enriched in a rat brain synaptic vesicle preparation. Ten micrograms of protein from brain microsomes (P2), synaptosomes (Syn), synaptic vesicles (SV), and postsynaptic densities (PSD) were probed on a western blot with TRPM7-CFP antibody. Synaptophysin was probed in the same samples as a marker of synaptic vesicles; a lysate of HEK 293T cells overexpressing TRPM7 (labeled M7) was used as a marker.

(B) Synaptic proteins synaptotagmin 1 (Syt1) and synapsin 1 (Syn1) coimmunoprecipitate with TRPM7. Solubilized rat brain synaptic vesicle preparations were immunoprecipitated (IP) with TRPM7-CFP antibody and probed on western blot with TRPM7-C47, Syt1, Syn1, and VAMP2 antibodies. The same preparation was immunoprecipitated with Syt1 and Syn1 antibodies and probed on western blot as indicated. Immunoprecipitation with normal rabbit immunoglobulins (IgG) is shown as a negative control. The same result was obtained when TRPM7 was immunoprecipitated with TRPM7-C47 antibody (not shown). X (% of sample used for IP and shown as input) = 2% for TRPM7, 1.5% for Syt1, 0.5% for Syn1, and 1.5% for VAMP2.

(C) TRPM7 is colocalized with the presynaptic marker, synaptophysin, in the neuromuscular junction. Confocal images of 5 μ sections of mouse gastrocnemius muscle demonstrate labeling with TRPM7-CFP antibody and anti-synaptophysin. DIC, differential interference contrast image.

(D) TRPM7 colocalizes with synaptophysin in synaptic varicosities of mature rat superior cervical ganglion (SCG) sympathetic neurons. Confocal images of sympathetic neurons 40 days in vitro were labeled with TRPM7-CFP antibody and anti-synaptophysin. TRPM7-C47 antibody labeling showed the same pattern and colocalization with synaptophysin (data not shown). TRPM7 antibody preabsorption with antigenic peptides suppressed the labeling (data not shown).

Alteration of TRPM7 Levels in Presynapses Affects Neurotransmission

So far, the data indicate that TRPM7 is located in the membrane of synaptic vesicles and interacts with

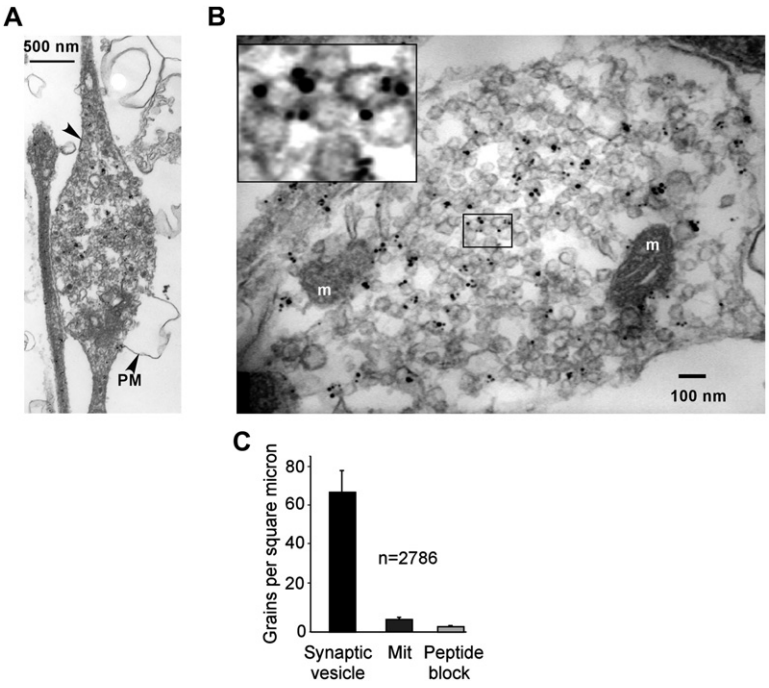

Figure 2. TRPM7 Is Expressed in the Membranes of Synaptic Vesicles of Cultured SCG Neurons

(A and B) Immunogold electron micrographs showing labeling of synaptic vesicles in neuronal process varicosities with TRPM7-CFP antibody. m, mitochondria; PM, plasma membrane. Insert displays magnified boxed area in (B).

(C) Statistical summary of the density of immunogold labeling of synaptic vesicles (± antigenic peptide block) and mitochondria (serving as a negative control). Data is from three independent labeled samples.

proteins that are known to be involved in synaptic vesicle exocytosis and neurotransmitter release—synapsin I (Chi et al., 2001), synaptotagmin I (Chapman, 2002), and snapin (Ilardi et al., 1999; Chheda et al., 2001). We hypothesized that the TRPM7 protein situated in the membrane of synaptic vesicles is involved in the regulation of neurotransmitter release. Amperometric detection of evoked catecholamine release with carbon fiber electrodes (Robinson et al., 1995) has been useful in sympathetic neurons (Zhou and Misler, 1995). However, in initial experiments with pheochromocytoma (PC12) cells, we found that TRPM7 specifically localized to small synaptic-like vesicles containing acetylcholine and was not expressed in dense core vesicles secreting catecholamines (data not shown). Since amperometry does not detect acetylcholine release, and since there is no evidence to suggest that these vesicles also contain catecholamines, we chose to measure excitatory postsynaptic potentials (EPSPs) from synaptically coupled neurons as an assay of synaptic vesicular release. To test the function of TRPM7 in synaptic vesicle release, we altered TRPM7 protein levels or channel activity in presynaptic neurons and measured EPSP amplitudes and kinetics in unaltered postsynaptic neurons.

Sympathetic neurons isolated from rat SCG were chosen as an experimental model since (1) TRPM7 is expressed in synaptic vesicles of SCG neurons in culture; (2) proteins are efficiently ectopically expressed in these neurons after DNA microinjection (Mochida et al., 2003); and (3) most adjacent neurons are connected by synapses, and recordings from neurons neighboring the stimulated neuron reproducibly yield cholinergic EPSPs (Mochida et al., 1994). First, we increased TRPM7 by overexpressing GFP-TRPM7; heterologous expression of GFP-TRPM7 in HEK 293T cells confirmed that the channel properties of this construct were indistinguishable of those for wild-type TRPM7 (data not shown). Second, TRPM7 synthetic siRNAs to rat TRPM7 (see Experimental Procedures) were employed to decrease levels of functional TRPM7 protein. In several model systems, TRPM7 siRNAs effectively knocked down TRPM7 protein levels. siRNAs cotransfected with rat TRPM7 into HEK 293T cells abrogated TRPM7 protein expression (Figure S2A). More than 90% of endogenous TRPM7 protein expression was suppressed in TRPM7-siRNA-transfected rat PC12 cells (Figure S2B). Finally, injected TRPM7-siRNA1 knocked down 40%, and TRPM7-siRNA2 nearly 90%, of endogenous TRPM7 protein in cultured rat SCG neurons used for electrophysiological recordings (Figure S2C).

Neurons were injected with GFP-TRPM7 cDNA or siRNA along with a GFP-expressing vector in order to visualize presynaptic neurons and assure that altered TRPM7 was presynaptically localized (Figure 3A). Action potentials were generated every 200 ms in presynaptic (GFP-labeled) neurons and EPSPs were recorded in adjacent synaptically coupled nontransfected neurons (modified Krebs' solution containing 0.2 mM $Ca^{2+}$and 5 mM Mg^{2+} was used in order to record release events of a few synaptic vesicles; Figure 3B).

The average EPSP amplitude recorded from postsynaptic neurons of TRPM7-overexpressing presynaptic neurons was 1.3-fold larger than in nontransfected synapses (2.26 ± 0.08 mV compared to 1.79 ± 0.06 mV). The average EPSP amplitudes were decreased to 64% of control levels by siRNA1 knockdown of TRPM7 (1.15 ± 0.05 mV, Figure 3C). Modulation of presynaptic TRPM7 resulted in prominent changes in postsynaptic EPSP amplitude histograms. TRPM7 overexpression increased the proportion of larger-amplitude EPSPs compared with controls, while siRNA1-induced TRPM7 knockdown increased the proportion of small-amplitude EPSPs (Figure 3F). Analysis of cumulative

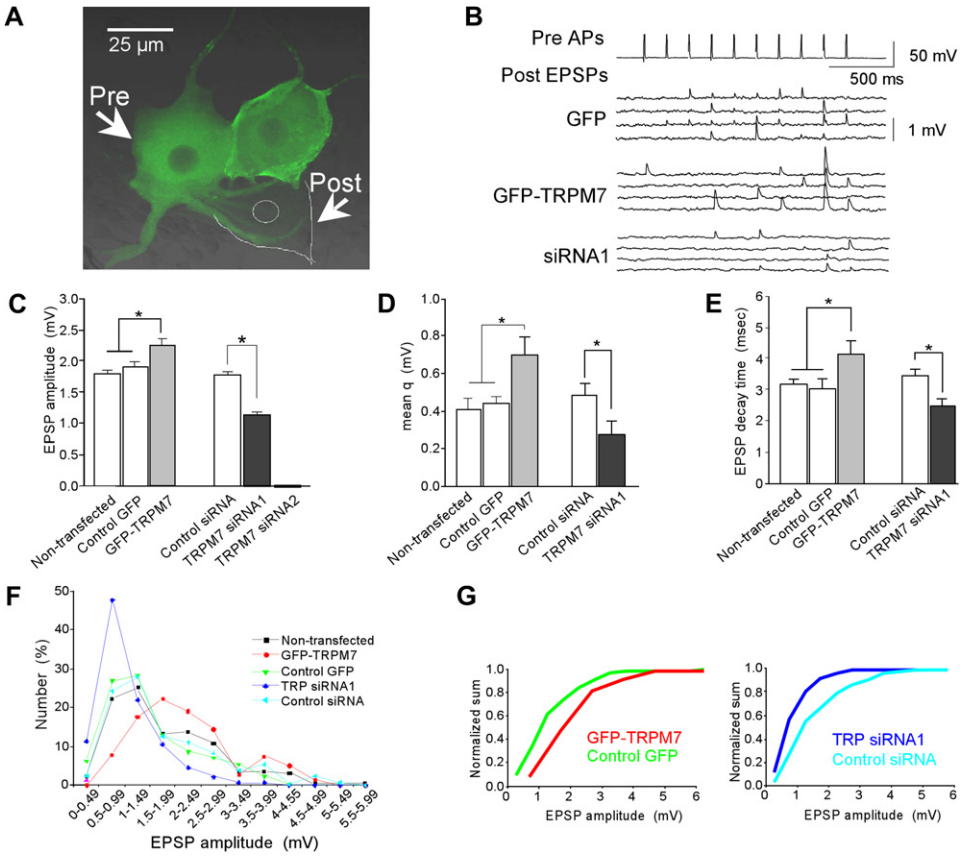

Figure 3. Presynaptic TRPM7 Levels Affect Synaptic Transmission between SCG Neurons in Culture

(A) Fluorescent image of SCG neurons transfected with GFP-TRPM7 (green) and a nontransfected neuron (outlined in white). Pre, presynaptic neuron; Post, postsynaptic neuron. Scale bar, 25 μm.

(B) Representative EPSPs recorded postsynaptically (Post EPSPs) in a modified Krebs' solution containing 0.2 mM Ca^{2+} and 5 mM Mg^{2+}. Presynaptic neurons were stimulated at 5 Hz to generate ten action potentials (Pre APs). The three sets of four traces are examples of postsynaptic responses from presynaptic neurons transfected by GFP only (GFP), GFP-TRPM7, and TRPM7 siRNA1, respectively.

(C) Mean amplitude of EPSPs in a modified Krebs' solution containing 0.2 mM Ca^{2+} and 5 mM Mg^{2+}. Fifty to one hundred and ten action potentials were generated in each synaptic pair of presynaptic neurons transfected with the construct indicated. Data recorded from nine to ten synapses (Non-transfected, 9; Control GFP, 9; GFP-TRPM7, 10; Control siRNA, 9; TRPM7 siRNA1, 10) are averaged for each bar (*$p < 0.05$, Student's unpaired t test). In total, 910 action potentials were evoked in presynaptic neurons transfected with each construct. In experiments with TRPM7 siRNA2-injected neurons, 20 action potentials were generated in each of 23 neuronal pairs and no EPSP was recorded.

(D) Mean quantal size (q) calculated by the variance of the amplitude of EPSP recordings as described in (C). Data for each construct were averaged (*$p < 0.05$, Student's unpaired t test).

(E) Mean decay time of EPSPs. Data measured by EPSP recordings as described in (C) were averaged for each bar (*$p < 0.05$, Student's unpaired t test).

(F) Amplitude histograms of EPSPs, evoked by 910 action potentials in presynaptic neurons transfected with the constructs indicated as described in (C) (Non-transfected, n = 224; GFP-TRPM7, n = 215; Control GFP, n = 253; TRPM7 siRNA, n = 134; and Control siRNA, n = 290).

(G) Cumulative amplitude histograms for EPSP recordings shown in (F). Control GFP-transfected (green) versus GFP-TRPM7 (red) or control siRNA (light blue) versus TRPM7 siRNA (dark blue). Histograms were significantly different at $p < 0.00001$ based on the Kolmogorov-Smirnoff test.

In all figures, data values represent mean ± SEM.

histograms showed that these differences were statistically significant (Figure 3G). To examine these effects in more detail, we carried out quantal analysis of EPSPs. According to the quantal release hypothesis, the efficacy of a synaptic connection depends on the size of the postsynaptic response to a quantum of the transmitter and the number of quanta released per action potential. Analysis showed that alteration of TRPM7 expression level mainly affected quantal size (Figure 3D), not quantal content (data not shown). This finding suggests that TRPM7 affects intrinsic properties of synaptic vesicle release, such as the amount of the releasable neurotransmitter (Rahamimoff and Fernandez, 1997) or the dynamics of the fusion pore (Burgoyne and Barclay, 2002; Pawlu et al., 2004).

EPSP kinetics were also affected by changes in TRPM7 protein expression. EPSP decay times were increased by presynaptic TRPM7 overexpression but decreased by presynaptic TRPM7 knockdown (Figure 3E). In nontransfected synapses, the mean decay time from peak to 2/3 of peak amplitude was 3.2 ± 0.2 ms. Presynaptic TRPM7 overexpression increased mean decay time by 1.3-fold to 4.1 ± 0.4 ms, while TRPM7 siRNA1 knockdown decreased decay times to 78% of control

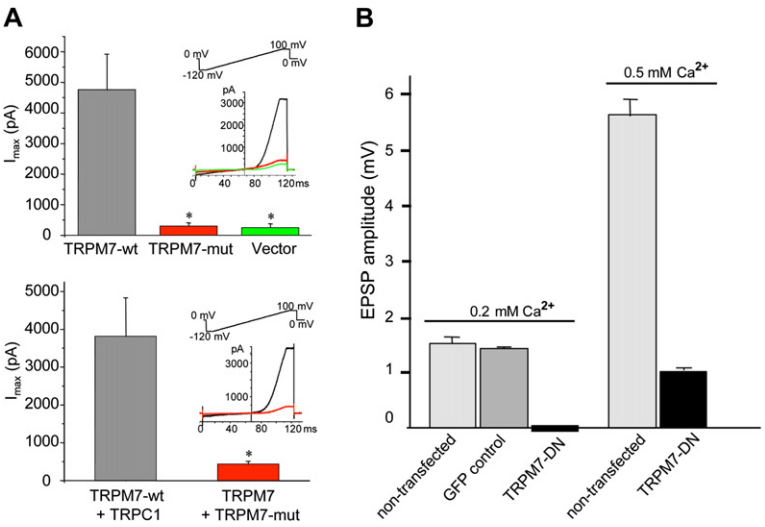

Figure 4. Dominant-Negative TRPM7 Mutant Abrogates Synaptic Transmission between SCG Neurons

(A) Wild-type GFP-TRPM7 (TRPM7wt) was coexpressed with a 5-fold excess of unlabeled TRPC1 or the pore mutant of TRPM7 (TRPM7mut). Expression of TRPC1 and TRPM7mut (both FLAG-tagged) in green (GFP) cells was confirmed by immunofluorescence. TRPM7mut abrogated TRPM7 current, acting as a dominant-negative subunit (TRPM7-DN). Each bar graph is the average current measured at +100 mV from six to eight cells.

(B) Expression of TRPM7-DN in cultured sympathetic neurons suppresses EPSPs. 1500 (6 × 250 pulses at 5 Hz) action potentials were generated in each synaptic pair of presynaptic neurons transfected with the construct indicated, and averages of 151 (nontransfected), 131 (control GFP), 73 (TRPM7-DN in 0.5 mM), and 250 (nontransfected in 0.5 mM Ca^{2+}) EPSPs were recorded in response to 250 action potentials. Data recorded from four to eight synapses were averaged. For the bar graph of TRPM7-DN in 0.2 mM Ca^{2+}, 20 action potentials were generated in five neuronal pairs and no EPSP was recorded.

levels (2.5 ± 0.2 ms). These data suggest that the kinetics of acetylcholine release from synaptic vesicles were altered by changes in TRPM7 levels in presynaptic terminals.

EPSP amplitudes, and especially the time courses of EPSPs, are affected by changes in the membrane properties of postsynaptic cells. It was important to test for such changes when TRPM7 levels were modulated in adjacent presynaptic neurons. Thus, we measured the resting potential, membrane resistance, membrane capacitance, and ACh responses in the postsynaptic neurons surrounding neurons injected with GFP-TRPM7 DNA or siRNA. No significant changes to postsynaptic neuron membrane properties or ACh receptor activation were observed under these conditions (Figure S3). Thus, the changes observed in the EPSP amplitude, quantal size, and decay times were associated with neurotransmitter release, since presynaptic, but not postsynaptic, TRPM7 levels were altered by cDNA or siRNA transfection.

In additional experiments, another TRPM7 siRNA (siRNA2) was transfected in the SCG neurons 5 days prior to recordings. This second siRNA was much more efficient than siRNA1, decreasing TRPM7 protein by >90% (Figure S2C). siRNA2 expression resulted in complete suppression of postsynaptic responses (0.2 mM Ca^{2+}; Figure 3C, n = 23 neurons). To verify that postsynaptic neurons coupled to the siRNA2-injected neurons were functionally active, the external [Ca^{2+}] was increased to 1 mM, whereupon small amplitude EPSPs from siRNA2-expressing synapses were observed (1.30 ± 0.13 mV, n = 8 pairs, data not shown). These EPSPs could not be compared to postsynaptic responses from control neurons under the same conditions, since at 1 mM $[Ca^{2+}]_o$, all postsynaptic neurons generated action potentials in response to repetitive presynaptic stimulation (control siRNA-transfected neurons; four pairs). These results confirm that TRPM7 is critical for SCG neurotransmitter release at physiological levels of external [Ca^{2+}].

TRPM7 Dominant-Negative Pore Mutation Suppresses Synaptic Transmission

Is ion conduction via the TRPM7 pore, not just the protein itself, relevant to TRPM7-dependent neurotransmitter release? To answer this question, pore residues of TRPM7 were mutated and the resulting mutants tested in heterologous expression. Mutation of highly conserved amino acids located in the 6th putative transmembrane domain (amino acids 1090–1092, NLL mutated to FAP; NP_067425) resulted in almost complete suppression of TRPM7 current (Figure 4A). Control experiments demonstrated that the mutation did not affect TRPM7 protein expression levels (not shown). Coexpression of the wild-type TRPM7 with mutant TRPM7 suppressed the WT channel (Figure 4A), while coexpression with a TRPC1 splice variant (which did not yield current by itself) did not affect TRPM7 current (Figure 4A). We conclude that the TRPM7 NLL>FAP mutation acts as a dominant-negative subunit that assembles with TRPM7 and forms a nonconducting channel protein.

Expression of the dominant-negative TRPM7 (TRPM7-DN) mutant in SCG neurons resulted in complete suppression of postsynaptic responses from transfected neurons (0.2 mM Ca^{2+}; Figure 4B). To verify that these postsynaptic neurons were functionally active, $[Ca^{2+}]_o$ was increased to 0.5 mM. Under these conditions, low amplitude EPSPs with an acceptable signal/noise ratio for data analysis could be recorded from TRPM7-DN-expressing synapses. Mean EPSP amplitude from these synapses was 21% of EPSP amplitude from nontransfected controls (Figure 4B). This suppression of synaptic transmission by dominant-negative TRPM7 subunits strongly suggests that TRPM7's ionic conductance is critical for neurotransmitter release.

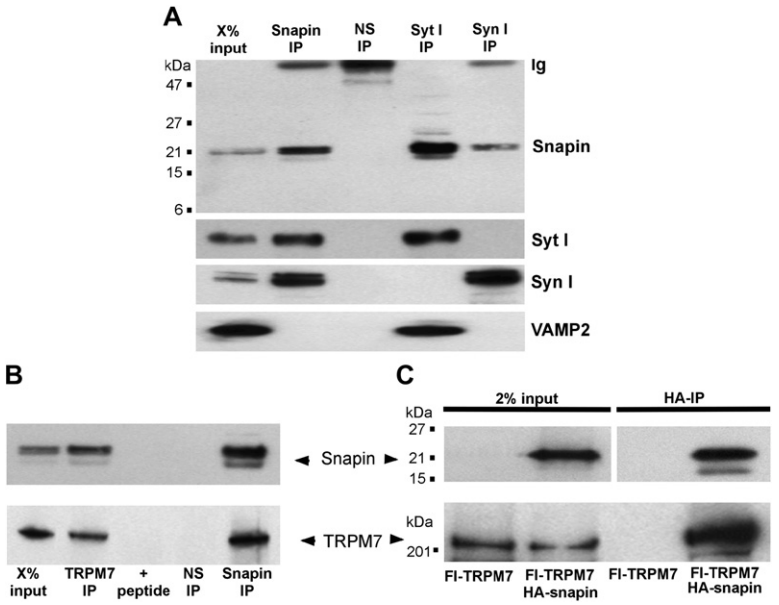

Figure 5. Native Snapin Binds Synapsin I, Synaptophysin I, and TRPM7

(A) Coimmunoprecipitation of synaptotagmin I (SytI) and synapsin I (SynI) with snapin from rat brain synaptic vesicles. Triton X-100 solubilized synaptic vesicle proteins were immunoprecipitated (IP) with anti-snapin antiserum, Syt1 and Syn1 antibody, or normal rabbit serum (NS) and probed on western blot with the antibody indicated. The data suggest that snapin is in a molecular complex with the synaptic vesicle-specific proteins synaptotagmin I and synapsin I. In these experiments, snapin did not coimmunoprecipitate synaptic vesicle-specific VAMP2 protein, serving as a negative control. X (% of sample used for IP and shown as input) = 4% for snapin, 0.6% for Syt1, 0.2% for Syn1, and 0.6% for VAMP2.

(B) TRPM7 and snapin cross-immunoprecipitate each other from purified synaptic vesicle lysates. Triton X-100 solubilized rat brain synaptic vesicle preparations were immunoprecipitated with TRPM7-C47 or snapin antibody and immunoprecipitates (IP) were probed on western blot with TRPM7-CFP (bottom panel) and snapin (top panel) antibodies. Immunoprecipitation with TRPM7 antibody pre-absorbed with antigenic peptide (+peptide) and with normal rabbit sera (NS), served as controls for specificity. X (% of sample used for IP and shown as input) = 2% for TRPM7, and 4% for snapin.

(C) Snapin coimmunoprecipitates TRPM7 from HEK 293T cells expressing two epitope-tagged proteins. FLAG-tagged full-length TRPM7 (Fl-TRPM7) and HA-tagged full-length snapin (HA-snapin) were expressed in HEK 293T cells and cell lysates were immunoprecipitated with anti-HA antibodies. Precipitates (HA-IP) and cell lysates (10 μg) were probed on western blot with anti-HA (HA-snapin) and anti-FLAG (Fl-TRPM7) antibodies.

The Functional Relevance of TRPM7's Interaction with Snapin

Since TRPM7 interacts with synaptic vesicle proteins involved in the vesicle fusion apparatus, specific disruption of this interaction might affect evoked neurotransmitter release. Our yeast two-hybrid results suggested that snapin and TRPM7 could directly interact. However, the synaptic localization of snapin has been disputed (Vites et al., 2004). To re-examine this issue, we tested whether endogenous snapin was in a molecular complex with synaptic vesicle-specific proteins. Snapin, immunoprecipitated from purified synaptic vesicles, bound the synaptic vesicle-specific proteins synapsin I and synaptotagmin I (Figure 5A). Complementary immunoprecipitation of synapsin I and synaptotagmin I also confirmed that snapin is in a molecular complex with these synaptic vesicle-specific proteins. In these experiments, the synaptic vesicle protein VAMP2 bound Syt1, but not TRPM7 or snapin, and thus VAMP2 served as a negative control (Figure 5A). These results confirm that snapin is indeed associated with synaptic vesicles.

To further examine whether TRPM7 is complexed with native snapin, we immunoprecipitated TRPM7 from a solubilized synaptic vesicle preparation. In these experiments, snapin was specifically coimmunoprecipitated with TRPM7 (Figure 5B). The interaction between TRPM7 and snapin was confirmed in a heterologous expression system. Full-length FLAG-tagged TRPM7 (coexpressed with HA-tagged snapin in HEK 293T cells and immunoprecipitated using FLAG antibody) coimmunoprecipitated snapin (Figure 5C).

To define the region of TRPM7-snapin interaction, in vitro translated 6xHis-tagged snapin peptide fragments and myc-tagged TRPM7 peptide fragments were labeled with [^{35}S]-methionine, and histidine-tagged snapin peptide fragments were pulled down with cobalt beads. The precipitated fragments were then detected by ^{35}S imaging. These experiments showed that amino acids 43–68 of snapin were sufficient to bind the TRPM7 N-terminal fragment (Figure 6A). The region of TRPM7 critical for snapin binding could not be further defined beyond that identified in the yeast two-hybrid assay (amino acids 87–326) because truncations of either the N or C termini of this peptide resulted in the loss of snapin binding (Figure 6B). This suggests that a 3D fold within amino acids 87–326 of TRPM7 is required for snapin binding.

We next tested whether TRPM7 and snapin directly bind each other by using purified peptide fragments of both proteins in an in vitro binding assay. Fusion proteins of TRPM7 (amino acids 87–326) and maltose binding protein (MBP-TRPM7$_{87–326}$) and fusion proteins of snapin (amino acids 43–68) and a 6xHis tag (6xHis-Snapin$_{43–68}$) were expressed in bacteria and affinity purified. Pull down of 6xHis-Snapin$_{43–68}$ with cobalt beads demonstrated that Snapin$_{43–68}$ specifically bound TRPM7$_{87–326}$ (Figure 6C). In control experiments, MBP itself did not bind 6xHis-Snapin$_{43–68}$ and cobalt beads alone did not bind MBP-TRPM7$_{87–326}$ (Figure 6C). Thus, if amino acids 43–68 of snapin are also critical in vivo for TRPM7-snapin complex stabilization, then a snapin peptide containing these amino acids should disrupt the TRPM7-snapin native complex. Indeed, a synthetic peptide comprised of these amino acids specifically disrupted the native TRPM7-snapin complex as tested by coimmunoprecipitation of the native molecules (Figure 6D). MBP-TRPM7$_{87–326}$ also specifically disrupted the native complex in the same assay

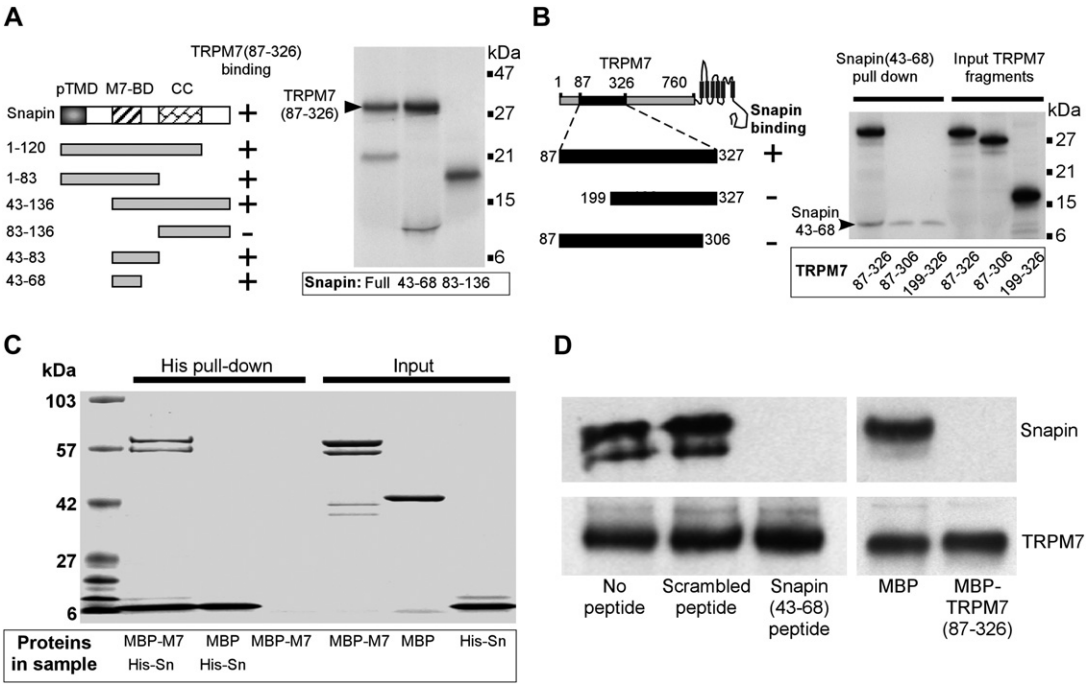

Figure 6. Defining the Snapin and TRPM7 Binding Domains

Diagrams depict the protein fragments of TRPM7 and the results of the binding assay. Images are [^{35}S]-autoradiograms of protein gels. Numbers designate amino acid sequences in full-length proteins. (A) 6xHis-tagged snapin and its fragments were translated in vitro with [^{35}S]-methionine, combined with in vitro translated [^{35}S]-TRPM7 (87–326), and precipitated with cobalt resin. The image shows that full-length snapin and the snapin peptide fragment (amino acids 43–68) bind the TRPM7 peptide fragment equally well. The nonbinding snapin peptide fragment (83–136) is shown as a negative control. Snapin structural domains are labeled thus: pTMD, putative transmembrane domain; M7-BD, TRPM7 binding domain; CC, coiled coil domain. (B) 6xHis-tagged [^{35}S]-snapin fragment containing amino acids 43–68 and fragments of [^{35}S]-TRPM7 were translated in vitro and precipitated with cobalt resin. "Input" displays the amount of in vitro translated fragments used in the pull-down assay. (C) Snapin directly binds TRPM7. Maltose binding protein (MBP) fusion with the TRPM7 peptide fragment (amino acids 87–326; MBP-M7) and 6xHis-snapin peptide fragment (amino acids 43–68; His-Sn) were expressed in bacteria and affinity purified. Point three micrograms of the proteins indicated were combined and 6xHis-snapin was pulled down with cobalt resin. In this Coomassie-stained gel, "Input" displays the amount of the purified protein used in the pull-down assay. Left lane, molecular markers. His, histidine. (D) The molecules comprising the TRPM7-snapin binding sites (synthetic snapin$_{43–68}$ peptide and purified MBP-TRPM7$_{87–326}$ protein) disrupted the native TRPM7-snapin complex. TRPM7 was immunoprecipitated from a rat brain synaptic vesicle lysate with or without 50 μM snapin$_{43–68}$ synthetic peptide, scrambled peptide with the identical amino acid composition, MBP-TRPM7$_{87–326}$, or MBP alone. Immunoprecipitated proteins were probed on western blot with snapin (top panel) and TRPM7 (lower panel) antibody.

(Figure 6D). These interaction-disrupting peptides are used to probe the functional relevance of the interaction between TRPM7 and snapin.

Presynaptic neurons were perfused intracellularly with the TRPM7-snapin disrupting peptide Snapin$_{43-68}$. After recording control EPSPs every 20 s for >30 min, Snapin$_{43–68}$ peptide was microinjected into presynaptic neurons. Snapin$_{43–68}$ injection correlated with a gradual decrease in the amplitude of evoked EPSPs (Figures 7A and 7B). Thirty minutes after the start of peptide injection, the mean EPSP amplitude decreased by 22% ± 7.7% (n = 5). In control injections, the scrambled peptide at the same concentration caused no significant change in EPSP amplitudes (+0.6% ± 8.4%; $p < 0.05$; Figure 7C). Snapin peptide injection also altered the time course of EPSPs (Figure 7Ab). The first order derivative of EPSP waveforms shown in Figure 7Ab, representing the rate of rise and fall for EPSPs, clearly shows that the peptide reduced the rate of rise of the EPSP and shortened the time to its peak amplitude. Similar inhibition of the EPSP amplitude was caused by injection of the snapin-binding TRPM7 fragment (MBP-TRPM7$_{87–326}$; Figures 7C and 7D). Injection of heat-denatured MBP-TRPM7$_{87–326}$ or MBP alone did not alter measured synaptic transmission. Thus, in vivo disruption of the TRPM7-snapin complex by two separate, complementary peptides impaired synaptic transmission in SCG neurons. That TRPM7 and snapin comprise a synaptic vesicle molecular complex, and specific in vivo disruption of this complex inhibits synaptic transmission, supports the hypothesis that TRPM7 plays a critical role in neurotransmitter release. The advantage of these peptide competition experiments, compared to TRPM7 overexpression or siRNA-dependent knockdown, is that they are acute and thus circumvent artifacts associated with long-term processes. We conclude that TRPM7 interaction with snapin is important for neurotransmitter release.

Discussion

We have shown that TRPM7 is localized to the membrane of synaptic vesicles in sympathetic neurons and forms molecular complexes with the synaptic vesicle proteins synaptotagmin I, synapsin I, and snapin. In sympathetic neurons, changes in TRPM7 levels were

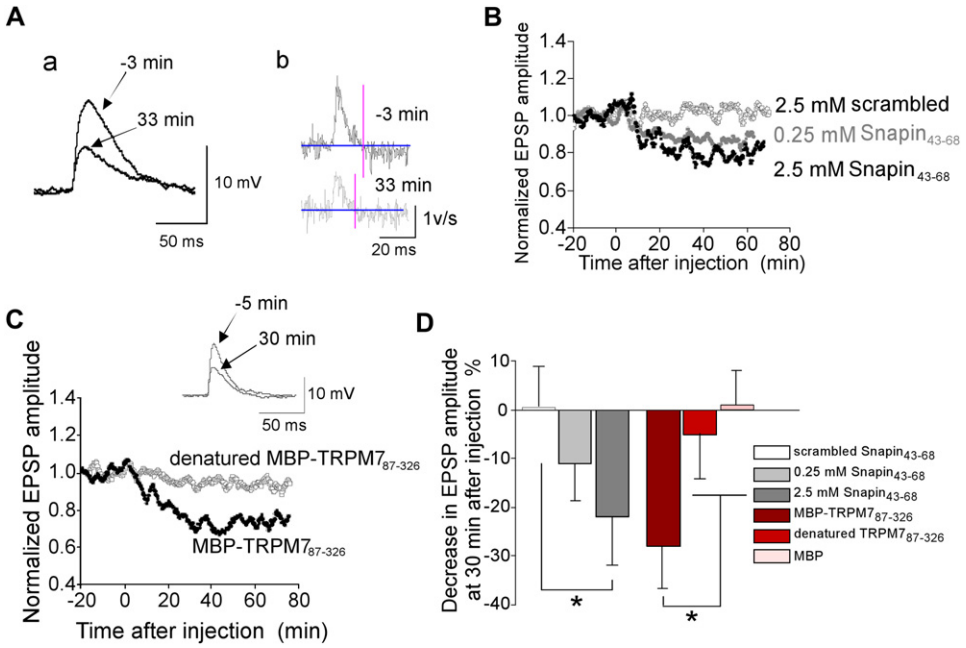

Figure 7. Disruption of the TRPM7-Snapin Native Complex Affects EPSP Amplitudes and Kinetics

(A) (Aa) EPSPs from one experiment recorded in a synapse before (−3 min) and after (33 min) snapin$_{43–68}$ injection. (Ab) The first order derivative of EPSPs shown in (Aa) shows the rate of rise and fall of the EPSP. The vertical marks (red) indicate the time to peak of the EPSP.

(B) Snapin$_{43–68}$ (0.25 or 2.5 mM in the pipette) or scrambled peptide (2.5 mM in the pipette) was injected into presynaptic neurons at time 0. Presynaptic neurons were stimulated every 20 s. Normalized EPSP amplitudes were averaged (n = 5 each). The resulting values were smoothed with a moving average algorithm (Experimental Procedures).

(C) MBP-TRPM$_{87–326}$ (n = 6) or denatured MBP-TRPM$_{87–326}$ (n = 5) (0.1 mM of each protein in pipette) was injected into presynaptic neurons at time 0. Insert displays EPSPs from one experiment recorded in a synapse before (−5 min) and after (30 min) protein injection.

(D) The mean reduction in EPSP amplitude at 30 min after the start of peptide injection (*$p < 0.05$ for 2.5 mM snapin$_{43–68}$ versus scrambled peptide, MBP-TRPM$_{87–326}$ versus denatured MBP-TRPM$_{87–326}$, or MBP alone by the Student's unpaired t test).

correlated with transmitter release as measured by changes in EPSP amplitudes and kinetics. The dominant-negative TRPM7 pore mutant expressed in SCG neurons substantially suppressed evoked neurotransmitter release, strongly suggesting that TRPM7's ionic conductance is critical for neurotransmitter release. Furthermore, we showed that changes in EPSP amplitudes depended on TRPM7's interaction with snapin. The molecular details of this interaction during vesicle fusion are unclear; it is possible that snapin is a scaffolding protein required for assembly of TRPM7 with other synaptic vesicle proteins, such as synapsin and synaptotagmin.

We hypothesize that TRPM7 functions as an ion conductance pathway across vesicular membranes that is crucial to transmitter release. Alterations in numbers of TRPM7 channels or their activity could modulate the amplitude and kinetics of EPSPs in several ways. Since TRPM7 was found in the synaptic vesicle membrane, but not in the plasma membrane, of the synaptic varicosities, the simplest conclusion is that ion flux via TRPM7 affects either synaptic vesicle-plasma membrane fusion or the amount of neurotransmitter released from a single vesicle. Calculation of quantal parameters from EPSPs suggested that TRPM7 alterations affected quantal size rather than the number of released vesicles and that TRPM7 vesicular current affects the amount of neurotransmitter released from a single synaptic vesicle. The amount of the neurotransmitter released from a single vesicle, or quanta, is not a constant value and is regulated by multiple signaling pathways (Burgoyne and Barclay, 2002). Consistent with our observation that TRPM7 affected EPSP kinetics, TRPM7 may affect quantal release size by altering pore fusion kinetics (Pawlu et al., 2004). Another possibility is that TRPM7 activity alters transvesicular voltage, which in turn may affect neurotransmitter release (Thevenod, 2002).

TRPM7 in a Model of Neurotransmitter Release from Synaptic Vesicles

TRPM7 might regulate the amount of mobile transmitter contained in a vesicle (Rahamimoff and Fernandez, 1997). This possibility is especially attractive since it predicts a critical role for the ion channel's conductance of ions across the vesicular membrane. Recent findings indicate that transmitters are immobilized in polymeric ion exchange gels inside vesicles (Nanavati and Fernandez, 1993; Reigada et al., 2003; Uvnas et al., 1989). To release neurotransmitter from the gel, counterions are required (Rahamimoff and Fernandez, 1997). The cation channel in the membrane of the synaptic vesicle would provide such counterions that could release positively charged neurotransmitters, such as acetylcholine. TRPM7 is well-suited for such a function since (1) it is a nonselective cationic channel; (2) it is outwardly rectifying and its orientation in the vesicle membrane provides prevailing cationic flow into the vesicle; and (3) TRPM7 channel opening requires PIP_2 (Runnels et al., 2002), which is lacking in prefusion synaptic vesicular membranes

(Holz et al., 2000; Micheva et al., 2001). The lack of PIP_2 suggests that TRPM7 is inactive before the vesicle associates with the plasma membrane. Vesicle attachment/fusion with the plasma membrane will bring vesicular TRPM7 into close proximity with PIP_2 in the plasma membrane, resulting in channel opening and cation flow into the vesicle; (4) TRPM7 activity is strongly activated at low extracellular pH (Jiang et al., 2005), corresponding to low vesicular intralumenal pH (Fuldner and Stadler, 1982). Fusion pore formation and communication with the external solution would dissipate the pH gradient and inactivate the channel.

The amount of diffusible neurotransmitter affects quantal size. If the number of vesicular channels providing counterions for neurotransmitter mobilization is limiting, then overexpression of the channel should increase quantal size and would result in an increase in EPSP amplitude, as observed in our experiments. Correspondingly, a decrease in the number of channels should decrease quantal size. Increased mobile neurotransmitter in the vesicle would also increase the duration of neurotransmitter release, resulting in an increase in EPSP decay time. In this model, channel activation, ion influx into the vesicle, and neurotransmitter mobilization occur *before* fusion pore formation. Cation influx could also rapidly increase vesicular osmotic pressure, favoring vesicle fusion.

In summary, TRPM7 proteins are in synaptic vesicles of sympathetic neurons and form a molecular complex with synaptic vesicle fusion machinery proteins. Ion conductance via TRPM7 is critical to neurotransmitter release in these cholinergic synaptic terminals. Colocalization of TRPM7 with synaptophysin in the neuromuscular junction implies a role for TRPM7 in neurotransmitter release in the synaptic terminals of motor neurons. Interestingly, other channels of the TRP superfamily, TRPV1 and TRPC3, also bind to several components of the vesicle fusion complex (Morenilla-Palao et al., 2004; Singh et al., 2004). Mucolipins of the TRPML subfamily (Di Palma et al., 2002; LaPlante et al., 2002) and TRPC5 (Bezzerides et al., 2004) have been studied in intracellular vesicle compartments as regulators of trafficking, but not as components of the vesicle fusion apparatus. The findings presented here may signal a role for other TRP channels in the mechanism of vesicular fusion.

Experimental Procedures

Yeast Two-Hybrid Screening

Sequences encoding the evolutionarily conserved domains of human TRPM7 were chosen using GenBank Blast searches. cDNAs encoding each domain were subcloned into the Gal4 binding domain fusion vector pGBKT7 (BD-Clontech). These constructs were used for screening the human brain library (Matchmaker pACT2, Clontech) expressed in AH109 yeast.

cDNA Constructs and Recombinant Proteins

We use the abbreviation GFP to refer to Enhanced Green Fluorescent Protein. FLAG-tagged mouse TRPM7 in pcDNA4TO was kindly provided by of Dr. Scharenberg (Univ. Washington). The N-terminal GFP-TRPM7 fusion protein was made from the above construct by insertion of GFP into the NotI site between the FLAG and TRPM7 sequences. Negative control TRPM7 plasmid was made from the GFP-TRPM7 construct by creating a stop codon after GFP. The TRPM7 mutation was made using the QuickChange protocol (Stratagene) and the mutated protein was completely sequenced. Human $TRPM7_{87–326}$ was subcloned into pMAL-c2X (New England Biolabs) and expressed as an MBP fusion in BL21 CodonPlus bacteria (Stratagene). The MBP fusion protein was affinity purified on amylose resin (New England Biolabs). For in vitro translation and mammalian cell expression, coding sequences or fragments of human TRPM7 and snapin were subcloned in frame in a modified pcDNA6 vector containing the N-terminal fusion protein for an HA- or FLAG-tagged sequence. His-HA-tagged snapin constructs were made by subcloning the corresponding PCR fragments into a modified 6xHis-HA vector containing the T7 promoter as described. Fusion peptides were expressed in BL21 CodonPlus bacteria (Novagen) and purified on an immobilized cobalt (Talon, Clontech) column. ^{35}S-labeled proteins were made with the T7-TNT system (Invitrogen) and [^{35}S]-methionine, according to the manufacturer's protocol (Amersham). Two synthetic double-stranded siRNAs were designed to the unique regions of rat TRPM7 (bases 975–995 [siRNA1] and 732–772 [siRNA2] of *AF375874*). Nonsilencing double-stranded RNA (Ambion) was used as a negative control.

Antibody, Immunoprecipitation, and Pull-Down Assays

Rabbit TRPM7 antibody (M7-CFP) was made against a glutathione S-transferase (GST) fusion peptide containing amino acids 1277–1393 of mouse TRPM7, and affinity purified on an immobilized β-galactosidase fusion peptide with the same TRPM7 sequence. The antibody recognized overexpressed TRPM7 on western blot and immunoprecipitated Flag-TRPM7 expressed in HEK 293T cells. The antibody was specific for immunofluorescent recognition of FLAG-TRPM7 expressed in COS-7 cells. A second rabbit TRPM7 antibody was described earlier (Runnels et al., 2002). Commercially available antibodies included rabbit snapin antibodies from Synaptic Systems (Göttingen, Germany); mouse synaptophysin (for western blot), mouse syntaxin, mouse FLAG (M2) antibodies from Sigma; mouse synapsin I (for western blot) antibody from BD Transduction; mouse HA antibody from Santa Cruz Biotechnology; mouse synaptotagmin I antibody from StressGen (Victoria, Canada); mouse synaptophysin antibody (for immunofluorescence; US Biological); Na,K-ATPase and PSD95 from ABR (Golden, Colorado), and rabbit synapsin I antibody (for immunoprecipitation) from Invitrogen (Zymed).

Transfected cells were solubilized in lysis buffer (50 mM Tris-Cl [pH 8.0], 150 mM NaCl, 1% Triton X-100) supplemented with a protease inhibitor cocktail (Complete, Roche), immunoprecipitated with the specified antibody, and washed with lysis buffer. Six- to eight-week-old rat brain P2 microsomes, synaptosomes, and postsynaptic densities were isolated (Carlin et al., 1980) and synaptic vesicles were purified (Phelan and Gordon-Weeks, 1997). Immunoprecipitation from the synaptic vesicle preparation was performed as described above for transfected cells. For TRPM7 antibodies used in immunoprecipitation experiments, negative controls were verified by antigen preabsorption. Also, all immunoprecipitating antibodies were tested for cross-reactivity with in vitro translated coimmunoprecipitated molecules. Both types of controls confirmed antibody specificity in immunoprecipitation assays and the absence of cross-reactivity of immunoprecipitating antibody. For pull-down assays, 5 μl of in vitro-translated or 2 μg purified proteins were incubated for 1 hr at 4°C with 10 μl cobalt resin in 300 μl RIPA buffer (20 mM Tris-Cl [pH 8.0], 150 mM NaCl, 1% Triton X-100, 0.5% Na-Cholate, 0.1% SDS-10 mM imidazole), washed with RIPA buffer, and solubilized in SDS sample buffer. Proteins were quantified using a modified Lowry assay (Sigma).

Immunofluorescence and Immunogold Procedures

Low-density rat SCG neurons without glial cells were plated on cover slips covered with collagen and grown for 40 days as described (Mahanthappa and Patterson, 2002). Neurons were fixed with 4% formaldehyde, permeabilized with 0.2% Triton X-100, and blocked by 10% goat serum and 1% BSA in PBS. 5 μm sections of formaldehyde-fixed rat gastrocnemius muscle were prepared as described (Drake et al., 1997). Sections were additionally fixed in 100% methanol, permeabilized, and blocked as above. Cy3-conjugated goat anti-rabbit IgG (Jackson ImmunoResearch Laboratories) and Alexa 488-conjugated goat anti-mouse IgG (Molecular Probes) were used as secondary antibodies. Images were acquired with an Olympus Fluoview-500 confocal microscope (60×, 1.4 N.A.

objective). For immunogold labeling, high-density rat SCG neurons were prepared on plastic coverslips as described below, except that the preparation was depleted of nonneuronal cells (Lockhart et al., 2000) and grown for 14 days. Cells were fixed with 4% formaldehyde plus 0.01% glutaraldehyde, permeabilized, and blocked as described above. After incubation with primary antibody, cells were decorated with goat anti-rabbit Fab fragments labeled with 1 nm gold particles (Nanogold) with silver enhancement (Nanoprobes).

Cell Cultures and Gene Expression

HEK 293T cells were grown in DMEM/F12 media supplemented with glycine, Na-hypoxanthine, penicillin/streptomycin, and 10% FBS. Cells were transfected using Lipofectamine 2000 (Invitrogen) and cultured for 48 hr.

Culture of SCG Neurons

Postnatal day 7 Wistar ST rats were decapitated under diethylether anesthesia according to the guidelines of the Physiological Society of Japan. Isolated SCG neurons were maintained in culture for 6 to 7 weeks as described (Mochida et al., 1994). In brief, SCGs were dissected, desheathed, and incubated with collagenase (0.5 mg/ml; Worthington Biochemical) in L-15 (Gibco) at 37°C for 10 min. Following enzymatic digestion, the semidissociated ganglion was triturated gently through a small-pore glass pipette until a cloudy suspension was observed. After washing by low-speed centrifugation at 1300 rpm for 3 min, the collected cells were plated onto coverslips in plastic dishes (Corning; 35 mm diameter, ~1 ganglion per dish) containing a growth medium of 84% Eagle's minimal essential medium, 10% fetal calf serum, 5% horse serum, 1% penicillin/streptomycin (Gibco Invitrogen), and 25 ng/ml nerve growth factor (2.5 S, grade II; Alomone Laboratories). Cells were maintained at 37°C in a 95% air, 5% CO_2-humidified incubator, and the medium was changed twice weekly.

Expression vectors and double stranded RNA (0.2–0.3 μg/μl), along with the dye Green FCF (3%, Sigma), were microinjected into SCG neurons through a micropipette (Mochida et al., 2003). siRNA was microinjected along with the GFP expression vector. Entry of the constructs into the cell was monitored by the intensity of the dye. The cells were maintained at 37°C in a 95% air, 5% CO_2-humidified incubator for 2 or 5 days (siRNA2 and DN), and the injected neurons were identified by GFP fluorescence with an inverted microscope (Diaphot 300, Nikon) equipped with epifluorescence. The injected neurons were examined as presynaptic neurons in paired neuronal recordings.

Synaptic Transmission between SCG Neurons

EPSPs were recorded as described (Mochida et al., 1996). Conventional intracellular recordings were made from two neighboring neurons using microelectrodes filled with 1 M KAc (70–90 MΩ). EPSPs were recorded from a nontransfected neuron while action potentials were generated in the GFP-expressing neurons by passage of current through an intracellular recording electrode. For Figure 3, five to ten recordings of EPSPs with ten stimuli at 5 Hz in nine to ten pairs (910 recordings in total) of each construct-transfected neuron were performed in a modified Krebs' solution consisting of 136 mM NaCl, 5.9 mM KCl, 0.2 mM $CaCl_2$, 5 mM $MgCl_2$, 11 mM glucose, and 3 mM Na-HEPES (pH 7.4). Extracellular Ca^{2+} and Mg^{2+} concentrations were 0.2 mM and 5 mM, respectively, in order to decrease the quantal content of evoked transmitter release (Del Castillo and Katz, 1954). Under these conditions three-fourths of presynaptic action potentials failed to produce EPSPs, indicating that the majority of EPSPs represented single, or a few, quantal events. Electrophysiological data were collected using software written by the late Dr. Ladislav Tauc (CNRS, France; Mochida et al., 1996) and analyzed with Origin 7.0 (Microcal Software) and the Mini Analysis Program 6.03 (Synaptosoft) for amplitudes and decay times of EPSPs. A Student's unpaired t test (two-tailed) was applied to compare EPSPs evoked by action potentials generated in transfected versus control neurons. The Kolmogorov-Smirnoff test was used to test the histograms (EPSP amplitude/number) for significance of effects from transfected synapses compared with control synapses. For Figure 4B, 6 × 250 action potentials at 5 Hz were applied. The data were collected by Clampex 9.2 (Axon Instruments) and analyzed with the Mini Analysis Program 6.03 (Synaptosoft). For the study of the effects of snapin and TRPM7 peptides, neurons were superfused with a modified Krebs' solution consisting of 136 mM NaCl, 5.9 mM KCl, 2.5 mM $CaCl_2$, 1.2 mM $MgCl_2$, 11 mM glucose, and 3 mM Na-HEPES (pH 7.4). Synaptic couples with subthreshold EPSPs were selected. Peptides were dissolved in 150 mM KAc, 5 mM Mg^{2+}-ATP, and 10 mM HEPES (pH 7.3) and introduced into the presynaptic cell body by diffusion from a glass suction pipette (15–20 MΩ tip resistance). Fast Green FCF (5%, Sigma) was included via the peptide injection solution to confirm entry into the presynaptic cell body. The injection pipette was removed 3 to 4 min after the start of the injection. The peak amplitudes of EPSPs were averaged and the resultant values were smoothed by an eight-point moving average algorithm and plotted against recording time with t = 0 indicating the start of presynaptic injection of peptides. The Student's unpaired t test (two-tailed) was applied to compare effects among presynaptic neurons injected with peptides. I-V curves were plotted using Clampex 9.2 (Axon Instruments).

Membrane input resistance was determined from the linear portion of three I-V curves and membrane input capacitance was calculated from the averaged membrane time constant and input resistance using Clampfit 9.2 (Axon Instruments). ACh responses were elicited by puff application of 5 μM ACh (3 psi, 20 ms) to a postsynaptic neuron every 5 s for 5 min. Data values with associated error, shown in the text and figures, represent mean ± SEM.

Quantal Analysis

Quantal analysis for postsynaptic potentials induced by action potentials generated in presynaptic neurons transfected with the TRPM7 constructs was performed using the variance method (Del Castillo and Katz, 1954). In this method, the quantal size (q, unitary response to a single quantum) and the quantal content (m, number of quanta released) are calculated by analyzing the distribution of a population of evoked EPSPs under the assumption that release of synaptic vesicle quanta follows a Poisson distribution. The mean (E) and standard deviation (σ) of this series of experiments were determined by the Mini Analysis Program 6.03 (Synaptosoft). The quantal content (m) was calculated from $m = 1/(cv)^2$, where $cv = \sigma/E$. The quantal size (q) was calculated from $q = E/m$.

TRPM7 Expression and Current Measurements in CHO-K Cells

CHO-K1 cells were transfected with 0.5–3 μg of cDNA as described above for HEK 293T cells. Whole-cell patch-clamp recording was performed 1 or 2 days posttransfection while cells were bathed in an extracellular solution containing, in mM, 130 NaCl, 5 CsCl, 1 $CaCl_2$, 10 Na-HEPES, and 10 glucose (pH 7.4). Patch pipettes pulled from borosilicate glass had resistances of ~2–4 MΩ when filled with the intracellular recording solution, consisting of, in mM, 125 Cs-methanesulfonate, 8 NaCl, 10 EGTA, 4.1 $CaCl_2$, and 10 HEPES (pH 7.4). Currents were recorded using an Axopatch 200A amplifier (Axon Instruments), filtered on-line at 2 kHz, sampled at an interval of 100 μs, and digitized using a Digidata 1322A and pClamp 9.2 software (Axon Instruments). Series resistance was <12.0 MΩ, and this was compensated by ~85% during experiments.

Supplemental Data

The Supplemental Data for this article can be found online at http://www.neuron.org/cgi/content/full/52/3/485/DC1/.

Acknowledgments

We thank Dr. Igor Medina for helpful discussion, S. Gapon and Y. Manasian for technical assistance, and E. Oancea for the GFP-TRPM7 construct. This work was supported by grants-in-aid for Scientific Research B and grants-in-aid for Scientific Research on Priority Areas (S.M.), and by the Howard Hughes Medical Institute (G.K. and D.E.C.).

Received: March 10, 2006
Revised: July 24, 2006
Accepted: September 18, 2006
Published: November 8, 2006

References

Bennett, M.R. (1972). Autonomic neuromuscular transmission. Monogr. Physiol. Soc. *30*, 1–271.

Bezzerides, V.J., Ramsey, I.S., Kotecha, S., Greka, A., and Clapham, D.E. (2004). Rapid vesicular translocation and insertion of TRP channels. Nat. Cell Biol. *6*, 709–720.

Buckley, K.M., and Landis, S.C. (1983). Morphological studies of synapses and varicosities in dissociated cell cultures of sympathetic neurons. J. Neurocytol. *12*, 67–92.

Burgoyne, R.D., and Barclay, J.W. (2002). Splitting the quantum: regulation of quantal release during vesicle fusion. Trends Neurosci. *25*, 176–178.

Buxton, P., Zhang, X.M., Walsh, B., Sriratana, A., Schenberg, I., Manickam, E., and Rowe, T. (2003). Identification and characterization of Snapin as a ubiquitously expressed SNARE-binding protein that interacts with SNAP23 in non-neuronal cells. Biochem. J. *375*, 433–440.

Carlin, R.K., Grab, D.J., Cohen, R.S., and Siekevitz, P. (1980). Isolation and characterization of postsynaptic densities from various brain regions: enrichment of different types of postsynaptic densities. J. Cell Biol. *86*, 831–845.

Chapman, E.R. (2002). Synaptotagmin: A Ca^{2+} sensor that triggers exocytosis? Nat. Rev. Mol. Cell Biol. *3*, 498–508.

Chheda, M.G., Ashery, U., Thakur, P., Rettig, J., and Sheng, Z.H. (2001). Phosphorylation of snapin by PKA modulates its interaction with the SNARE complex. Nat. Cell Biol. *3*, 331–338.

Chi, P., Greengard, P., and Ryan, T.A. (2001). Synapsin dispersion and reclustering during synaptic activity. Nat. Neurosci. *4*, 1187–1193.

Clapham, D.E. (2003). TRP channels as cellular sensors. Nature *426*, 517–524.

Del Castillo, J., and Katz, B. (1954). Quantal components of the end-plate potential. J. Physiol. *124*, 560–573.

Di Palma, F., Belyantseva, I.A., Kim, H.J., Vogt, T.F., Kachar, B., and Noben-Trauth, K. (2002). Mutations in Mcoln3 associated with deafness and pigmentation defects in varitint-waddler (Va) mice. Proc. Natl. Acad. Sci. USA *99*, 14994–14999.

Drake, C.T., Bausch, S.B., Milner, T.A., and Chavkin, C. (1997). GIRK1 immunoreactivity is present predominantly in dendrites, dendritic spines, and somata in the CA1 region of the hippocampus. Proc. Natl. Acad. Sci. USA *94*, 1007–1012.

Ehrenstein, G., Stanley, E.F., Pocotte, S.L., Jia, M., Iwasa, K.H., and Krebs, K.E. (1991). Evidence for a model of exocytosis that involves calcium-activated channels. Ann. N Y Acad. Sci. *635*, 297–306.

Fuldner, H.H., and Stadler, H. (1982). 31P-NMR analysis of synaptic vesicles. Status of ATP and internal pH. Eur. J. Biochem. *121*, 519–524.

Grahammer, F., Herling, A.W., Lang, H.J., Schmitt-Graff, A., Wittekindt, O.H., Nitschke, R., Bleich, M., Barhanin, J., and Warth, R. (2001). The cardiac K^+ channel KCNQ1 is essential for gastric acid secretion. Gastroenterology *120*, 1363–1371.

Greengard, P., Benfenati, F., and Valtorta, F. (1994). Synapsin I, an actin-binding protein regulating synaptic vesicle traffic in the nerve terminal. Adv. Second Messenger Phosphoprotein Res. *29*, 31–45.

Holz, R.W., Hlubek, M.D., Sorensen, S.D., Fisher, S.K., Balla, T., Ozaki, S., Prestwich, G.D., Stuenkel, E.L., and Bittner, M.A. (2000). A pleckstrin homology domain specific for phosphatidylinositol *4*, 5-bisphosphate (PtdIns-4,5-P2) and fused to green fluorescent protein identifies plasma membrane PtdIns-4,5-P2 as being important in exocytosis. J. Biol. Chem. *275*, 17878–17885.

Ilardi, J.M., Mochida, S., and Sheng, Z.H. (1999). Snapin: a SNARE-associated protein implicated in synaptic transmission. Nat. Neurosci. *2*, 119–124.

Jackson, V.M., and Cunnane, T.C. (2001). Neurotransmitter release mechanisms in sympathetic neurons: past, present, and future perspectives. Neurochem. Res. *26*, 875–889.

Jentsch, T.J., Neagoe, I., and Scheel, O. (2005). CLC chloride channels and transporters. Curr. Opin. Neurobiol. *15*, 319–325.

Jiang, J., Li, M., and Yue, L. (2005). Potentiation of TRPM7 inward currents by protons. J. Gen. Physiol. *126*, 137–150. Published online July 11, 2005. 10.1085/jgp.200409185.

Kelly, M.L., and Woodbury, D.J. (1996). Ion channels from synaptic vesicle membrane fragments reconstituted into lipid bilayers. Biophys. J. *70*, 2593–2599.

LaPlante, J.M., Falardeau, J., Sun, M., Kanazirska, M., Brown, E.M., Slaugenhaupt, S.A., and Vassilev, P.M. (2002). Identification and characterization of the single channel function of human mucolipin-1 implicated in mucolipidosis type IV, a disorder affecting the lysosomal pathway. FEBS Lett. *532*, 183–187.

Lockhart, S.T., Mead, J.N., Pisano, J.M., Slonimsky, J.D., and Birren, S.J. (2000). Nerve growth factor collaborates with myocyte-derived factors to promote development of presynaptic sites in cultured sympathetic neurons. J. Neurobiol. *42*, 460–476.

Mahanthappa, N.K., and Patterson, P.H. (2002). Culturing mammalian sympathoadrenal derivatives. In Culturing Nerve Cells, Second Edition, G. Banker and K. Goslin, eds. (Cambridge, MA: Bradford Book), pp. 289–308.

Micheva, K.D., Holz, R.W., and Smith, S.J. (2001). Regulation of presynaptic phosphatidylinositol 4,5-biphosphate by neuronal activity. J. Cell Biol. *154*, 355–368.

Mochida, S., Nonomura, Y., and Kobayashi, H. (1994). Analysis of the mechanism for acetylcholine release at the synapse formed between rat sympathetic neurons in culture. Microsc. Res. Tech. *29*, 94–102.

Mochida, S., Sheng, Z.H., Baker, C., Kobayashi, H., and Catterall, W.A. (1996). Inhibition of neurotransmission by peptides containing the synaptic protein interaction site of N-type Ca^{2+} channels. Neuron *17*, 781–788.

Mochida, S., Westenbroek, R.E., Yokoyama, C.T., Itoh, K., and Catterall, W.A. (2003). Subtype-selective reconstitution of synaptic transmission in sympathetic ganglion neurons by expression of exogenous calcium channels. Proc. Natl. Acad. Sci. USA *100*, 2813–2818.

Morenilla-Palao, C., Planells-Cases, R., Garcia-Sanz, N., and Ferrer-Montiel, A. (2004). Regulated exocytosis contributes to protein kinase C potentiation of vanilloid receptor activity. J. Biol. Chem. *279*, 25665–25672.

Nanavati, C., and Fernandez, J.M. (1993). The secretory granule matrix: a fast-acting smart polymer. Science *259*, 963–965.

Palmer, C.P., Zhou, X.L., Lin, J., Loukin, S.H., Kung, C., and Saimi, Y. (2001). A TRP homolog in Saccharomyces cerevisiae forms an intracellular Ca(2+)-permeable channel in the yeast vacuolar membrane. Proc. Natl. Acad. Sci. USA *98*, 7801–7805.

Pawlu, C., DiAntonio, A., and Heckmann, M. (2004). Postfusional control of quantal current shape. Neuron *42*, 607–618.

Phelan, P., and Gordon-Weeks, P.R. (1997). Isolation of synaptosomes, growth cones and their subcellular components. In Neurochemistry, A Practical Approach, Second Edition, A.J. Turner and H.S. Bachelard, eds. (Oxford, New York, Tokyo: IRL Press), pp. 27–33.

Rahamimoff, R., and Fernandez, J.M. (1997). Pre- and postfusion regulation of transmitter release. Neuron *18*, 17–27.

Ramsey, I.S., Delling, M., and Clapham, D.E. (2006). An introduction to TRP channels. Annu. Rev. Physiol. *68*, 619–647.

Reigada, D., Diez-Perez, I., Gorostiza, P., Verdaguer, A., de Aranda, I.G., Pineda, O., Vilarrasa, J., Marsal, J., Blasi, J., Aleu, J., and Solsona, C. (2003). Control of neurotransmitter release by an internal gel matrix in synaptic vesicles. Proc. Natl. Acad. Sci. USA *100*, 3485–3490.

Robinson, I.M., Finnegan, J.M., Monck, J.R., Wightman, R.M., and Fernandez, J.M. (1995). Colocalization of calcium entry and exocytotic release sites in adrenal chromaffin cells. Proc. Natl. Acad. Sci. USA *92*, 2474–2478.

Runnels, L.W., Yue, L., and Clapham, D.E. (2002). The TRPM7 channel is inactivated by PIP(2) hydrolysis. Nat. Cell Biol. *4*, 329–336.

Singh, B.B., Lockwich, T.P., Bandyopadhyay, B.C., Liu, X., Bollimuntha, S., Brazer, S.C., Combs, C., Das, S., Leenders, A.G., Sheng, Z.H., et al. (2004). VAMP2-dependent exocytosis regulates plasma

membrane insertion of TRPC3 channels and contributes to agonist-stimulated Ca^{2+} influx. Mol. Cell *15*, 635–646.

Stobrawa, S.M., Breiderhoff, T., Takamori, S., Engel, D., Schweizer, M., Zdebik, A.A., Bosl, M.R., Ruether, K., Jahn, H., Draguhn, A., et al. (2001). Disruption of ClC-3, a chloride channel expressed on synaptic vesicles, leads to a loss of the hippocampus. Neuron *29*, 185–196.

Sudhof, T.C. (2002). Synaptotagmins: why so many? J. Biol. Chem. *277*, 7629–7632. Published online December 5, 2001. 10.1074/jbc.R100052200.

Sudhof, T.C. (2004). The synaptic vesicle cycle. Annu. Rev. Neurosci. *27*, 509–547.

Thakur, P., Stevens, D.R., Sheng, Z.H., and Rettig, J. (2004). Effects of PKA-mediated phosphorylation of Snapin on synaptic transmission in cultured hippocampal neurons. J. Neurosci. *24*, 6476–6481.

Thevenod, F. (2002). Ion channels in secretory granules of the pancreas and their role in exocytosis and release of secretory proteins. Am. J. Physiol. Cell Physiol. *283*, C651–C672.

Uvnas, B., Aborg, C.H., Lyssarides, L., and Danielsson, L.G. (1989). Intracellular ion exchange between cytoplasmic potassium and granule histamine, an integrated link in the histamine release machinery of mast cells. Acta Physiol. Scand. *136*, 309–320.

Vites, O., Rhee, J.S., Schwarz, M., Rosenmund, C., and Jahn, R. (2004). Reinvestigation of the role of snapin in neurotransmitter release. J. Biol. Chem. *279*, 26251–26256. Published online April 14, 2004. 10.1074/jbc.M404079200.

Yakir, N., and Rahamimoff, R. (1995). The non-specific ion channel in Torpedo ocellata fused synaptic vesicles. J. Physiol. *485*, 683–697.

Zhou, Z., and Misler, S. (1995). Amperometric detection of stimulus-induced quantal release of catecholamines from cultured superior cervical ganglion neurons. Proc. Natl. Acad. Sci. USA *92*, 6938–6942.